Stimulus Artifact Cancellation in the Serosal Recordings of Gastric Myoelectric Activity Using Wavelet Transform

Hualou Liang*, *Senior Member, IEEE,* and Zhiyue Lin, *Senior Member, IEEE*

***Abstract*—Previous studies have shown that electrical stimulation of the stomach (i.e., gastric pacing) with appropriate parameters is a promising method for treatment of gastroparetic patients. The recording of gastric myoelectric activity (GMA) by serosal electrodes is often used to evaluate the effect of stimulation. However, the major problem with the measurement of GMA during gastric pacing is the stimulus artifacts which are often superimposed on the serosal recording and make analysis difficult. The frequency-domain adaptive filter has been used to reduce the stimulus artifacts but only with limited success. This paper describes a wavelet transform-based method for the reduction of stimulus artifacts in the serosal recordings of GMA. The key of this method lies in the use of the fuzzy set theory to select the stimulus artifact-related modulus maxima in the wavelet domain. Both quantitative and qualitative measures show that significant stimulus artifact cancellation was achieved through a series of computer simulations. Results from both single- and multichannel serosally recorded myoelectric signals during gastric pacing are presented to demonstrate the efficiency of the proposed method for the cancellation of stimulus artifacts.**

***Index Terms*—Fuzzy logic, gastric pacing, stimulus artifacts, wavelet transform.**

I. Introduction

As in the human heart, there is a gastric pacemaker in the stomach which is located in the midcorpus along the greater curvature. It generates a so-called slow wave propagating distally toward the pylorus (Fig. 1). The gastric slow wave is omnipresent and its normal frequency in humans is about 0.05 Hz. The frequency and propagation of gastric contractions are determined by the gastric slow wave. Spikes, bursts of rapid changes in gastric myoelectric activity (GMA), are directly associated with antral contractions. The antral muscles contract when slow waves are superimposed with spike potentials [1], [2]. Abnormalities in GMA may result in gastric motility disorders, such as gastroparesis. Gastroparesis is defined as delayed gastric emptying of a solid meal. Since gastric motility is regulated by GMA, abnormalities in GMA may lead to delayed gastric emptying [3], [4]. Recent studies have shown that electrical stimulation, or pacing, of the stomach may become a possible treatment approach for gastric motor dysfunctions [5], [6].

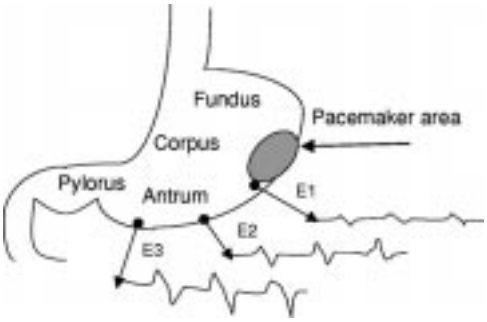

Fig. 1. Diagram of gastric pacemaker and electrical activity in different regions of the stomach.

Electrical stimulation of the human stomach, like pacing of the human heart, is achieved by externally delivering electrical currents via electrodes positioned in the certain position of the stomach. In practice, several pairs of electrodes are often implanted on the serosa of the stomach so that one can be used for delivering electrical currents and others for recording GMA. The major problem with the measurement of GMA during gastric pacing is the stimulus artifacts (SA) which are often superimposed on the serosal recording [see Fig. 2(a)]. Since the electrodes used for delivering the electrical stimuli are positioned close to the recording electrodes, the SAs sometimes comprise a large portion of the recorded signals. The SAs, usually consisting of periodic rectangular pulses, have overlapped frequency components with the gastric myoelectric signal and, therefore, cannot be eliminated by using conventional low-pass or bandpass filters or simply by subtraction of the SAs from the original recording [7]. The frequency-domain adaptive filter has been used to reduce the SAs but only with limited success [7]. The time-frequency representation has previously been employed in the analysis of nonstationary electrical signals of the stomach [8]. For review, see [9]. However, in the presence of stimulation artifacts, frequency analysis of serosal recordings during gastric pacing is unreliable. Therefore, advanced signal processing methods are needed to cancel the SAs in the severely distorted gastric signals.

The wavelet transform (WT) has emerged as an exciting new tool for statistical signal and image processing. The wavelet domain provides a natural setting for many applications involving biomedical signals, such as electrocardiogram analysis

Manuscript received March 6, 2001; revised March 8, 2002. *Asterisk indicates corresponding author.*

*H. Liang is with the Center for Computational Biomedicine, School of Health Information Sciences, The University of Texas Health Science Center, 7000 Fannin, Suite 600, Houston, TX 77030 USA (e-mail: hualou.liang@uth.tmc.edu).

Z. Lin is with the University of Kansas Medical Center, Department of Medicine, Kansas City, Kansas 66160 USA.

Publisher Item Identifier S 0018-9294(02)05775-0.

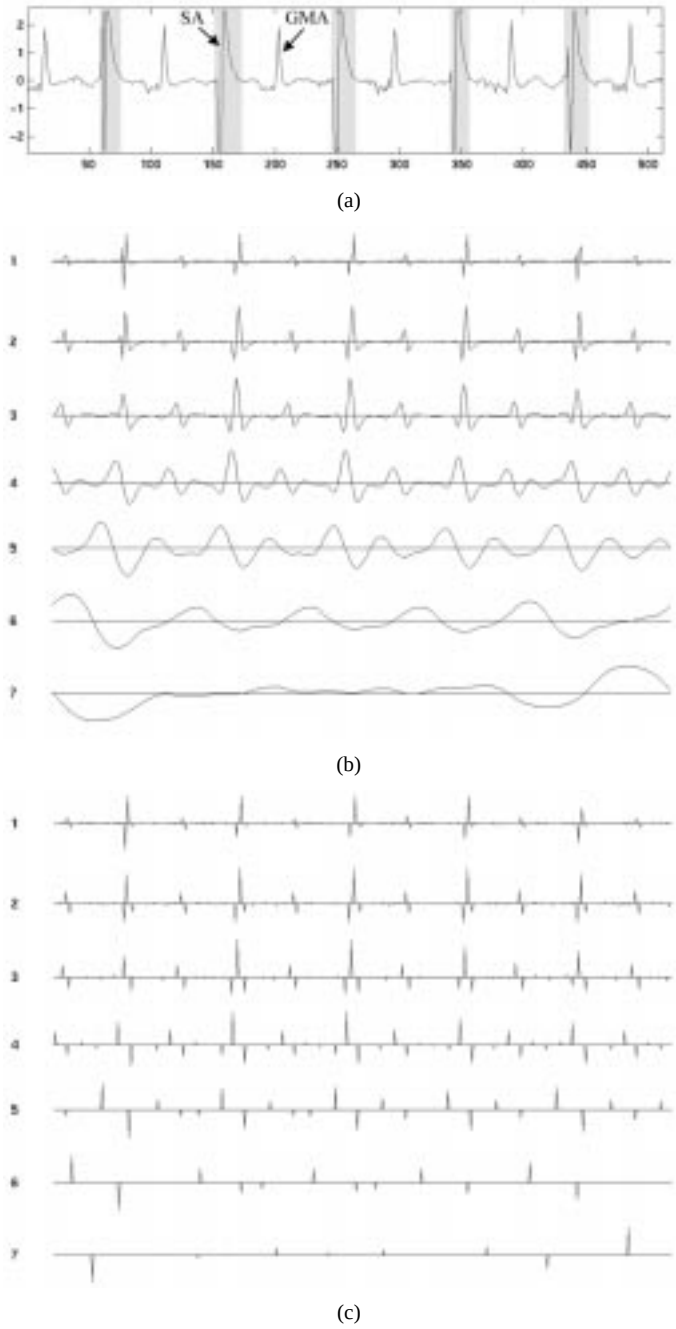

Fig. 2. (a) A serosal recording with gray bars indicating the SA and the remaining part belonging to the GMA, (b) WT of the signal shown in (a) computed with the quadratic spline wavelet at seven scales and (c) WTMM. At each scale, each Dirac indicates the position of a modulus maximum and the value of the WT at the corresponding location.

[10], [11], edge detection of medical image [12], classification [13], and chronobiological signal [14]. The remarkable properties of the WT have led to powerful signal processing methods based on simple scalar transformations of individual wavelet coefficients. The objective of the present study is to examine the applicability of the WT for canceling SAs in gastric myoelectric recordings. The key point in the canceling SAs in the recording is how to select wavelet coefficients representing gastric signal and eliminate the ones related to SAs. We describe a fuzzy-based technique for selecting the desired modulus maxima (MM) in wavelet domain, then using them to reconstruct the gastric signal.

II. The Wavelet Transform (WT)

The continuous WT (CWT) of a one-dimensional signal $x(t) \in L^2(R)$ with respect to a mother wavelet $\psi(t)$ is defined as [15], [16]

$$W_x(a,b) = \frac{1}{\sqrt{|a|}} \int_{-\infty}^{+\infty} x(t)\psi\left(\frac{t-b}{a}\right) dt \qquad (1)$$

where a, b ($a, b \in \mathcal{R}$ and $a \neq 0$) are the scale and translation parameters, respectively. The CWT $W_x(a,b)$ gives a time-scale decomposition (where the scale can be considered as similar in functionality to frequency) of the signal $x(t)$ with a indexing the scale and b indexing time in the original signal space. Dilated versions of $\psi_{a,b}(t)$ will match low-frequency components and on the other hand, contracted versions will match high-frequency oscillations. Hence, the CWT exhibits the property of "zooming" in on the sharp temporal variations in a signal.

The main disadvantages of the CWT are redundancy and computational complexity. In practice, the WT scale and translation parameters are discretized and for fast numerical implementation the scale normally varies along a dyadic sequence $(2^s)_{s\in Z}$. This yields the *Dyadic WT* [17]:

$$W_x(s,n) = \frac{1}{\sqrt{2^s}} \int_{-\infty}^{+\infty} x(t)\psi\left(\frac{t-n}{2^s}\right) dt \qquad (2)$$

For a wavelet centered at time zero and frequency f_0, the wavelet coefficient $W_x(s,n)$ characterizes the signal $x(t)$ around the time n and frequency $2^{-s}f_0$.

In this paper, the realization of the dyadic WT follows with that of Mallat's approach [17], [18]. The mother wavelet we used is a quadratic spline wavelet, due to its similarity with the SA. It is the first derivative of the cubic spline function. In fact, there are many different functions suitable as wavelets, each having different characteristics that are more or less appropriate depending on the application. Irrespective of the mathematical properties of the wavelet to choose, a basic requirement is that it looks similar to the patterns we want to localize in the signal. This allows a good localization of the structures of interest in the wavelet domain.

Having chosen the quadratic spline wavelet as the mother wavelet, it can be shown that the WT, $W_x(s,n)$, is proportional to the first derivative of the low-pass filtered version of signal $x(t)$ [18]. As a consequence, for any given scale s, the MM and modulus minima of the WT $W_x(s,n)$ correspond, respectively, to the points of sharp variation and slow variation of the smoothed signal at scale s. Thus, the local shape of irregular structures in the signal can be characterized by the evolution of wavelet local maxima across scales. This multiscale characterization of the signal was called by Mallat *et al.* [17], [18] the WTMM representation. The WTMM is used to describe any point (s_0, n_0) such that $|W_x(s,n)|$ is a locally maximum at $n = n_0$. This implies that

$$\frac{\partial W_x(s_0,n_0)}{\partial n} = 0. \qquad (3)$$

This local maximum should be a strict local maximum in either the right or the left neighborhood of n_0, to avoid having any local maxima when $|W_x(s_0,n)|$ is constant. Fig. 2 demonstrates the multiscale decomposition of a signal. Fig. 2(a) gives an example of a serosal recording during gastric pacing. Fig. 2(b) shows its WT computed at seven scales, whereas the Fig. 2(c) shows the corresponding MM of the WT. The WTMM representation of a signal records the values and locations of local maxima of its WT modulus. In [18], it is showed that a signal could be reconstructed, with good approximation, from the WTMM. For details of the description of the WTMM representation and the efficient implementation of the reconstruction algorithm, refer to the original work [17], [18].

III. Methods

A. Experimental Methods

1) Placement of Serosal Electrodes: The data used in this study were obtained in nine gastroparetic patients who participated in a trial on electrical stimulation of the stomach to aid gastric emptying [6]. Four pairs of temporary cardiac pacing wires (A & E Medical, Farmingdale, NJ) were implanted on the serosal surface of the stomach along the greater curvature from the corpus to pylorus during the scheduled surgery for the placement of the feeding jejunostomy tube. The distance between adjacent pairs of electrodes was 4 cm. The most distal electrodes were 2–4 cm above the pylorus. The electrodes were affixed to the gastric surface by partially embedding the wire in the seromuscular layer of the stomach. The wires were brought out through the abdominal wall percutaneously and placed under a sterile dressing.

2) Measurement of GMA: The study on gastric pacing was performed one week or more after the surgical procedure. Electrical stimulation was delivered via the most proximal electrodes using a commercial available stimulator (WPI, New Haven, CT). The electrical stimuli consisted of periodic rectangular pulses with an amplitude of 4 mA, width of 0.3 s, and frequency of 10% higher than the intrinsic gastric slow wave frequency. GMA was recorded from the electrodes distal to the pacing electrodes during the entire study. All signals were recorded on a tape recorder. For the computerized data analysis, all recorded signals were played back from the tape recorder and low-pass filtered at 0.5 Hz and then digitized at 10 Hz.

B. Cancellation of SAs Using WT

The serosally recorded gastric myoelectric signal during gastric pacing mainly consists of gastric slow waves, SAs and a considerable amount of noise due to muscular and respiratory activities, etc. The key to cancel the SAs from gastric myoelectric recordings using WT is how to select the desired WT coefficients for reconstruction of gastric slow waves. This is the choice of which coefficients to keep and which to eliminate. Our solution lies in the use of the fuzzy set theory and associated operators [19] to extract gastric slow waves related maxima in wavelet domain, which has been shown its efficacy for the edge detection of medical image [12] and the extraction of fetal electrocardiogram (ECG) [11].

As stated, the SAs contained in the serosal recordings result from an external pulse generator. The SAs may differ from the stimuli in magnitudes and locations, but the information about locations of the stimuli is steadily available. Such *a priori* information can be best exploited with the fuzzy set theory to accommodate the time ambiguity (the uncertainty of location) of SAs in reference to the stimuli. The time ambiguity, arising mostly from the time delay of propagation, is the main motivation to take advantage of fuzzy membership functions.

Specifically, the MM locations, with some ambiguity, are compared at each scale between the stimuli and the gastric myoelectric recording during pacing. A triangular fuzzy membership function, $\mu(s,n)$, centered on the maxima location n at scale s, is employed to represent the time ambiguity. The fuzzy intersection between two fuzzy sets, $\mu_p(s,n)$ and $\mu_g(s,n)$ of the stimuli and the gastric myoelectric recording during pacing, respectively, corresponds to the locations of the MM of SAs, which can be expressed as

$$M_{pg}(s,n)=\begin{cases}\mu_p(s,n)\cap\mu_g(s,n), & \text{if } n \text{ is a local maximum}\\ 0, & \text{elsewhere.}\end{cases} \tag{4}$$

The $M_{pg}(s,n)$ consists of the membership values in the interval [0,1]. Its complementary set, $M_{\bar{pg}}(s,n)$, indexing to the locations of the MM of the GMA is, therefore, written as

$$M_{\bar{pg}}(s,n)=\begin{cases}1-M_{pg}(s,n), & \text{if } n \text{ is a local maximum}\\ 0, & \text{elsewhere.}\end{cases} \tag{5}$$

The fuzzy decision is finally made to form the desired MM of the GMA, as follows:

$$W_g^m(s,n)=W_x^m(s,n)\times M_{\bar{pg}}(s,n) \tag{6}$$

where $W_x^m(s,n)$ denotes the MM of the WT $W_x(s,n)$. Fig. 3 illustrates the above fuzzy decision making procedure. The essence of the fuzzy-based technique is to determine the fuzzy intersection between the stimulus and the SA contained in the gastric myoelectric recording in their WTMM representations so that it provides tolerance with respect to their misalignments in the MM.

Let us remark a critical point when implementing the fuzzy-based algorithm. This is the choice of triangular fuzzy membership function. The width of the membership function at the lowest scale was empirically set to be two samples on each side of the MM, which gave us good results. Once the fuzziness width at the lowest scale is determined, it must be proportionally varied by a factor of two with the scale to ensure more uncertainty at the higher scales. The choice of the proportional factor of two is due to the use of dyadic WT where the evolution of a single point across scales falls with the *cone of influence*. The *cone of influence* of x_0 for any scale s is defined by $|x-x_0|\le Ks$ [17], where K is the support of the mother wavelet. Its definition clearly reveals that the neighborhood of x_0 proportionally varies with the scale.

From the above analysis, we design a four-stage procedure for the SA cancellation as follows.

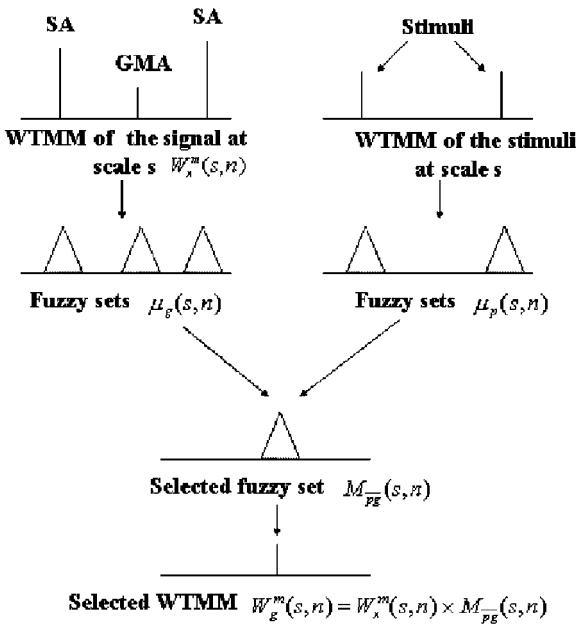

Fig. 3. Fuzzy decision making schema for estimation of the MM of gastric myoelectrical signal. For a given scale s, the top two plots show the WTMM of the gastric myoelectric recording during pacing (top left) and the stimuli (top right). Underneath (second row) are their corresponding triangular fuzzy functions. The complementary set of their fuzzy intersections is labeled in the third row as the selected fuzzy set belonging to the GMA. The MM of gastric myoelectrical signal (last row) are then selected by applying the selected fuzzy set on the WTMM of the gastric myoelectric recording during pacing (top left).

- *Analysis stage:* WTMM representations of the serosal recordings and of the stimuli in the time-scale plane are obtained using WT.
- *Denoising stage:* For the WTMM representation of the serosal recordings, the local maxima with amplitudes below certain threshold for each scale are removed, where the threshold is adaptive determined with the scale-dependent threshold estimation procedure called SureShrink [20].[1] The SureShrink, derived from minimizing Stein's unbiased risk estimate, is data-driven adaptive thresholding method and has been shown to perform well. It was showed in [17] that the WTMM curves of the noise decay across scales at least at a rate of $1/2^s$ or even do not propagate to larger scales. Consequently, in application of denoising, we can remove noise of a signal by removing all the WTMM of which the amplitude decreases when the scale increases. This step is expected to remove noise and thus reduce spurious spikes contained in the signal which could be otherwise mistaken as SAs.
- *Estimation stage:* The MM of the gastric myoelectric signal is estimated using a fuzzy-based technique, as detailed above.
- *Reconstruction stage:* The gastric myoelectric signal is reconstructed from the estimated MM [18].

The procedure we described so far is for one-channel SA cancellation. Application to multichannel recordings is straightforward by applying the above procedure for each channel recorded since the SAs contained in all the channels are generated by the same pulse generator. Once the MM of SAs is extracted, such information can be repeatedly used to cancel SAs by other channels where available.

[1]Comparisons with other two frequently used scale-dependent threshold estimation procedures (VisuShrink and Minimax) [21] were also made, with the SureShrink yielding slightly better result over the wide signal-to-noise (SNR) range.

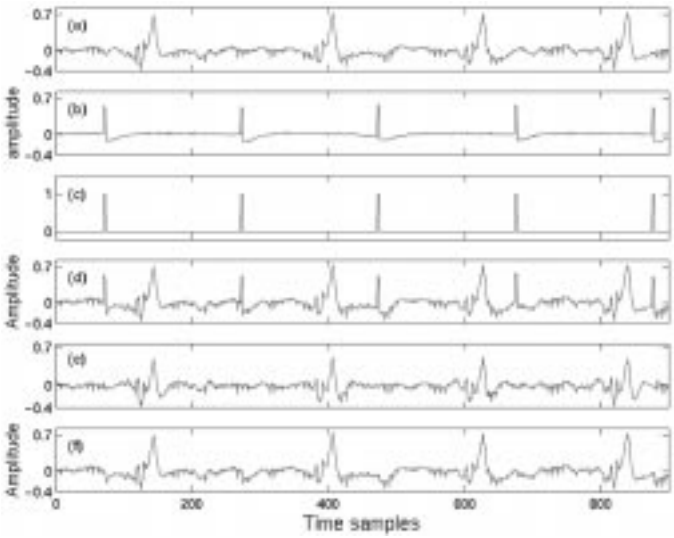

Fig. 4. The simulation example of cancellation of the SA. (a) A segment of clean gastric myoelectrical signal. (b) SAs taken from the most proximal electrode. (c) The stimuli as *a priori* consisting of periodic rectangular pulses with width of three samples (0.3 s at the sampling frequency of 10 Hz) and amplitude of one. (d) The synthesized composite signal using (a) and (b). (e) The reconstructed gastric myoelectrical signal by the proposed method. (f) The reconstructed gastric myoelectrical signal by the time-domain gating method.

1) Computational Complexity: The computational complexity (in terms of multiplications) of the proposed approach at each stage is described as follows. At the analysis stage, the WT with the implementation of a filter bank is of the order of $O(N \log_2 N)$ [17], [18], where N is the number of signal samples. The numerical complexity of the denoising stage, i.e., the SureShrink computation, is $O(N \log_2 N)$ [20]. At the estimation stage, the fuzzy-based selection of MM of gastric myoelectric signal requires $O(N \log_2 N)$ operations [11]. The reconstruction algorithm usually takes less than ten iterations to converge with good approximation (a mean-square error on the order of 10^{-2}). Each iteration is done with an $O(N \log_2 N)$ number of computation [18]. Hence, the total computational complexity of the proposed procedure is of the order of $O(10N \log_2 N)$.

IV. Performance Analysis

A series of computer simulations was conducted to investigate the performance of the proposed algorithm. Simulated signals include: 1) a clean serosal recording as shown in Fig. 4(a), which is free of SAs, obtained before the delivery of the external electrical simulation; 2) a stimulus signal taken from the most proximal electrode, representing SAs shown in Fig. 4(b); and 3) a series of white Gaussian noise with different noise levels to simulate the noise interference in the recording. Both qualitative (visual) and quantitative measures were used to assess the effectiveness of the proposed procedure. The root-mean-square error (RMSE) between the clean serosal recording, $x(n)$ and the

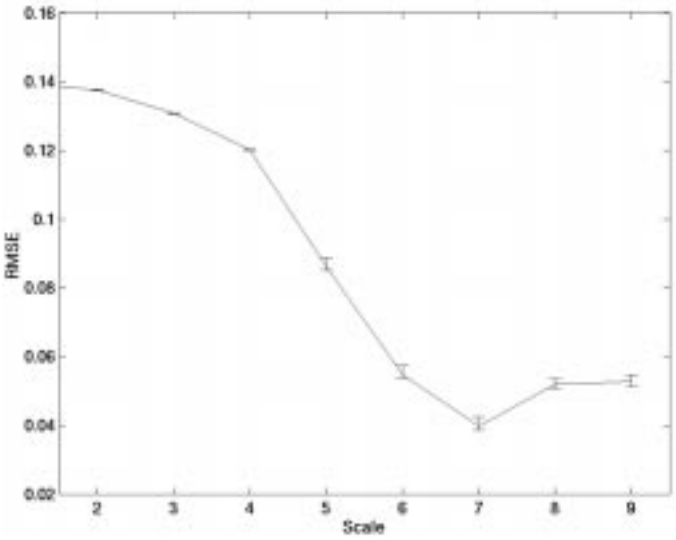

Fig. 5. The RMSE between the clean gastric myoelectric signal and the reconstructed one changed with scales. The error bars were obtained from an ensemble of 100 synthesized signals with a given clean gastric myoelectric signal and the SA varied systematically by multiplying a constant from 0.01 to 1.0, with the increment of 0.01. The minimum RMSE is achieved at $s = 7$.

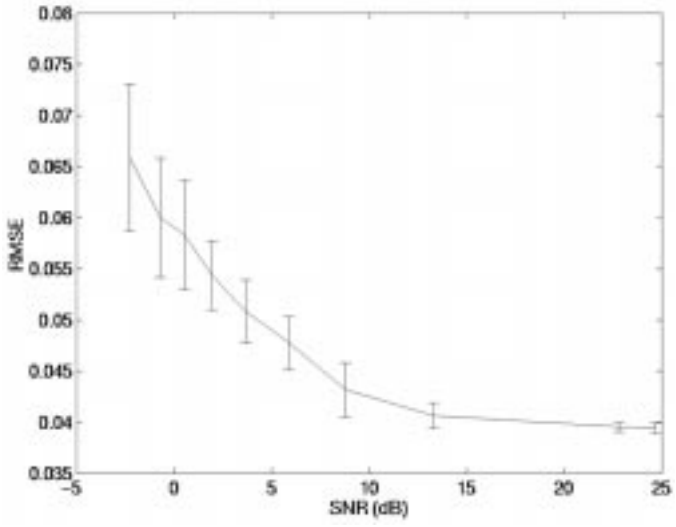

Fig. 6. The RMSE between the clean gastric myoelectric signal and the reconstructed one plotted against SNR with error bars obtained from 100 independent experiments.

extracted gastric slow wave, $\hat{x}(n)$, served as a merit measure, which is computed as

$$\mathrm{RMSE} = \sqrt{\frac{1}{N}\sum_{n=1}^{N}(x(n) - \hat{x}(n))^2}. \tag{7}$$

A. Effect of the Scales of the Wavelet Decomposition

For a discrete signal of length N, the maximum number of available scales in the wavelet decomposition is defined as $S = \log_2^N$. The number of scales s is usually chosen to be $\log_2^N$. However, it has been proven that the choice of s depends on the signals [17]. We construct a composite signal [Fig. 4(d)] of the clean gastric myoelectric signal [Fig. 4(a)] and the SA [Fig. 4(b)] to explore the effect of the scale. The stimuli are shown in Fig. 4(c). Once the very first location of SA has been identified, the stimuli can be generated on the basis of electrical stimuli consisting of a series of periodic rectangular pulses with width of 0.3 s (three samples at the sampling frequency of 10 Hz) and amplitude of one. We note that the amplitude of the stimulus can be any value since the only relevant information of the stimulus in the proposed method is its location. The RMSE between the clean GMA and reconstructed one as a function of the scale is shown in Fig. 5, where the RMSE first decreases up to scale seven, then increases as the scale s becomes larger. The error bars were obtained from 100 composite signals generated in such a way that, given the clean gastric myoelectric signal, the SA was varied systematically by multiplying a constant from 0.01 to 1.0, with the increment of 0.01. In our application, $s = 7$ was found to be a good choice. An example of the reconstructed gastric myoelectric signal is shown in Fig. 4(e). It is clear that the SA is substantially reduced.

B. Effect of Additive Noise

The effect of additive noise on the performance of the proposed procedure was studied as follows. A simulated signal was composed of a clean gastric myoelectric signal, SA, and white noise. For different noise levels, the signal-to-noise ratio (SNR) was calculated with respect to the energy of the gastric myoelectric signal. For the given noise level (or the given SNR), 100 independent experiments were conducted. The RMSE with error bars was plotted against SNR in Fig. 6. It may be noted that the SA can be canceled with acceptably low RMSE unless the SNR falls to low levels where the SA is indiscernible.

V. Comparative Study

In this section, we compare the performance of the proposed algorithm with that of the time-domain gating method [7]. The time-domain gating method is a simple technique currently used for the cancellation of SA. Basically, the SA is first determined by the threshold method and was then subtracted from the gastric myoelectric recording. An example is shown in Fig. 4(f). Since the commonly used quantitative method for gastric myoelectric signal is the power spectral analysis we, therefore, plot the power spectra as shown in Fig. 7, in which the spectra of the clean gastric myoelectric signal [Fig. 4(a)], the composite signal [Fig. 4(d)], the reconstructed gastric myoelectric signal [Fig. 4(e)] by the proposed method, and that [Fig. 4(f)] by the time-domain gating method are shown in thin solid, dashed, thick solid and dash-dotted lines, respectively. We can see from these curves that the spectrum of the reconstructed gastric myoelectric signal by the proposed method is close to that of the clean gastric myoelectric signal, whereas the time-domain gating method results in large deviation, particularly around the fundamental frequency (0.05 Hz) of the gastric slow wave.

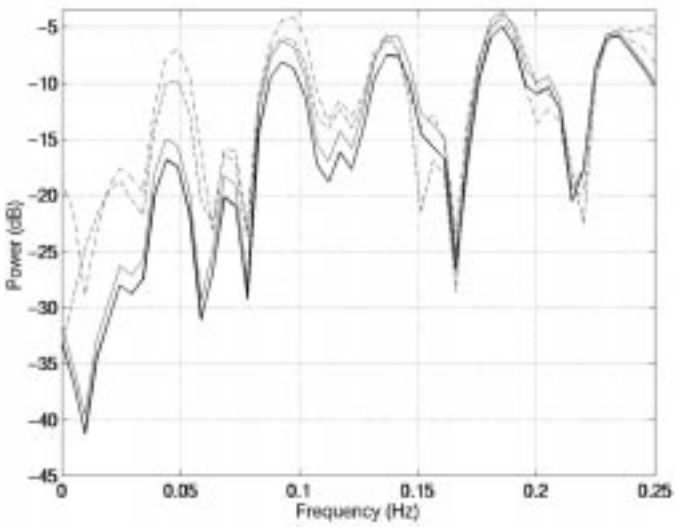

Fig. 7. Comparison of power spectra of the clean gastric myoelectric signal (thin solid line), the composite signal (dashed line), the reconstructed gastric myoelectric signal by the proposed method (thick solid line) and that by the time-domain gating method (dash-dotted line).

To quantitatively assess the performance of the proposed method, we compute the following relative error defined as follows:

$$\delta = \frac{\sum_{f} [P(f) - P'(f)]^2}{\sum_{\bar{f}} P^2(\bar{f})}$$

where $P(f)$ and $P'(f)$ are, respectively, the spectral densities of the clean and the reconstructed gastric myoelectric signals, f indexes the normal GMA ranging from 0.04 to 0.062 Hz, and $\bar{f}$ ranges from 0.0083 to 0.15 Hz. This relative error measures the degree of the waveform distortion relative to the clean gastric myoelectric signal. Indeed, the proposed method yields smaller relative error (0.0027 ± 0.003) than that of time-domain gating method (0.0371 ± 0.001). The standard deviations were obtained from 100 repetitions through adding white noise in the composite signals with the SNR of 10 dB.

VI. Experimental Results

The experimental data obtained from nine patients during gastric pacing were used in this study. Results from both single- and multichannel recordings are reported here. Substantial cancellation of the SAs in the serosal recording was achieved using the proposed procedure. A typical serosal recording during gastric pacing is presented in Fig. 8(a). The reconstructed gastric signal is depicted in Fig. 8(b). We can see from Fig. 8 that the most dominant characteristics of gastric signal are well preserved after the cancellation of SAs.

To further illustrate the effectiveness of the proposed method, a segment of serosal recording from a patient with dysrhythmia was selected. Fig. 9 shows the original recording [Fig. 9(a)] and the extracted gastric signal [Fig. 9(b)]. It can be seen that the proposed method performs equally well as previous examples in spite of the high irregularity of the gastric signal. This is mainly due to the fact that the method only takes advantage of the locations of SAs. As long as the locations of SAs remain relatively invariant, it will be able to cancel SAs from the gastric myoelectric recordings.

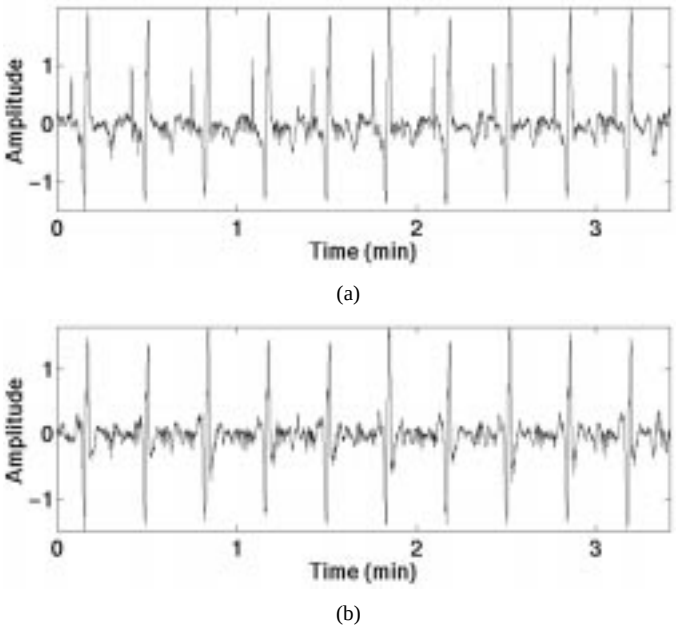

Fig. 8. A result of cancellation of SAs. (a) Serosal recordings during gastric pacing. (b) Reconstructed gastric myoelectrical signal.

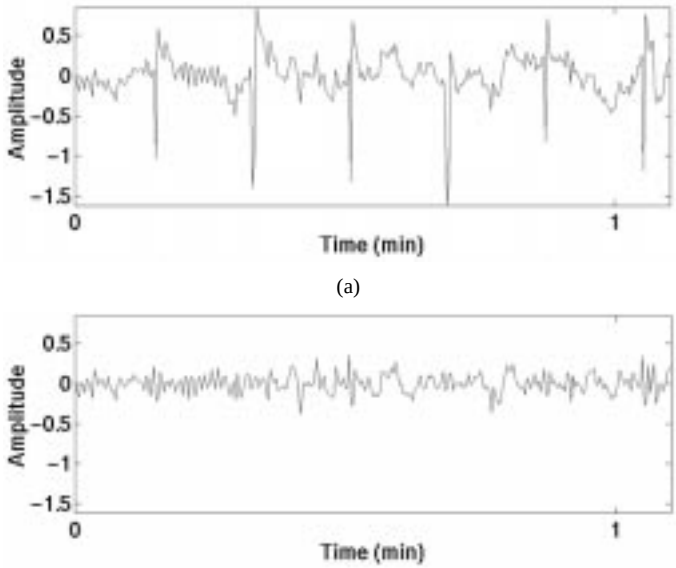

Fig. 9. Cancellation of SAs of the serosal recording obtained from a patient with dysrhythmia. (a) Serosal recording. (b) Reconstructed gastric myoelectrical signal.

One example of applications to the multichannel recordings is presented in Fig. 10. In Fig. 10, we show three-channel recordings during gastric pacing [Fig. 10(a)] and corresponding extracted gastric signals [Fig. 10(b)]. It is clearly observed that the SAs in the recordings are greatly reduced.

VII. Discussion and Summary

The WT has been applied for the cancellation of the SAs in the serosal recording of GMA. The performance of the pro-

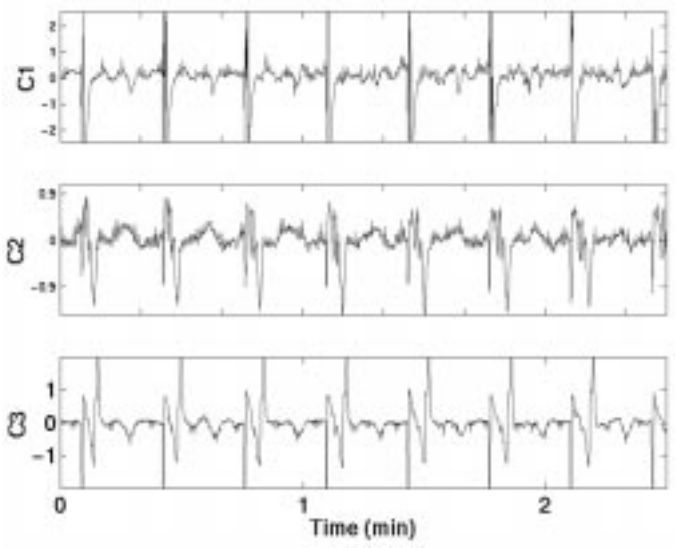

(a)

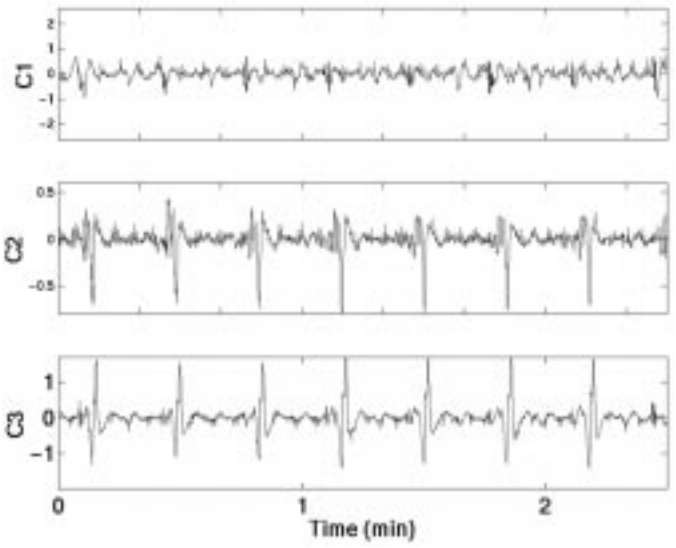

(b)

Fig. 10. Cancellation of SAs in the multichannel recordings. (a) Three-channel recordings during gastric pacing. (b) Reconstructed gastric myoelectrical signals.

posed method was investigated through a series of computer simulations. Results on both single and multichannel recordings demonstrate the effectiveness of the proposed method. The analysis is based on the robust identification of locations of the MM of SAs in serosal recordings in the wavelet domain, which is achieved by taking advantage of the stimuli as the *a prior* information to determine the locations and the fuzzy set theory to accommodate their uncertainties. The efficiency of the algorithm stems mainly from the fact that the locations of SAs remain relatively invariant with respect to various sources of noise.

Owing to the fact that the real stimulus signal is a multicomponents signal and that the electrodes for recording of the GMA are positioned close to the electrode for delivering the stimuli, the SAs superimposed on the real serosal recording are generally large in amplitude and overlapped with the frequency of the gastric myoelectric signal. Therefore, neither conventional bandpass filters nor the direct subtraction can be applied to eliminate SAs. The frequency-domain adaptive filter has been used to reduce the SAs but only with limited success [7]. Other techniques such as slew rate limiting [22] are suitable for artifact suppression in the neuromuscular investigation, but it is not as easily applicable to that in the GMA where the stimuli consist of periodic rectangular pulses.

While applying the proposed algorithm to cancel SAs in the serosal recordings, two practical aspects deserve further remarks. First, if the SAs coincided with the gastric slow waves, the algorithm would not work well. However, it is not likely in most cases that both of their singularities are completely overlapped both in scale and in time. Second, if there are spikes in the serosal recording of GMA, their MM similar to those of the SA will also propagate to higher scales, which will be mistaken as SAs. This problem needs further analysis.

ACKNOWLEDGMENT

The authors would like to thank Dr. J. Z. Chen and Dr. R. W. McCallum for their guidance in data collection.

REFERENCES

[1] S. K. Sarna, "Gastrointestinal electrical activity: Terminology," *Gastroenterology*, vol. 68, pp. 1631–1635, 1975.
[2] R. A. Hinder and K. A. Kelly, "Human gastric pacemaker potential: Site of origin, spread and response to gastric transection and proximal gastric vagotomy," *Amer. J. Surg.*, vol. 133, pp. 29–33, 1978.
[3] T. L. Abell, M. Camilleri, V. S. Hench, and J.-R. Malagelada, "Gastric electromechaniecal function and gastric emptying in diabetic gastroparesis," *Eur. J. Gastroenterol. Hepatol.*, vol. 3, pp. 163–167, 1991.
[4] J. D. Z. Chen, Z. Y. Lin, and R. W. McCallum, "Abnormal gastric myoelectric activity and delayed gastric emptying in patients with symptoms suggestive of gastroparesis," *Dig. Dis. Sci.*, vol. 41, pp. 1538–1545, 1996.
[5] B. O. Familoni, T. L. Abell, D. Nemoto, G. Voeller, A. Salem, and O. Gabor, "Electrical stimulation at a frequency higher than basal rate in human stomach," *Dig. Dis. Sci.*, vol. 42, pp. 885–891, 1997.
[6] R. W. McCallum, J. D. Z. Chen, Z. Y. Lin, B. D. Schirmer, R. D. Williamms, and R. A. Ross, "Gastric pacing improves emptying and symptoms in patients with gastroparesis," *Gastroenterology*, vol. 114, pp. 456–461, 1998.
[7] Z. Y. Lin and R. W. McCallum, "Adaptive stimulus artifact cancellation in the gastric myoelectric signals," in *Proc. 20th Ann. Int. Conf. IEEE Eng. Med. Bio. Soc.*, 1998, pp. 1636–1639.
[8] Z. Y. Lin and J. D. Z. Chen, "Time-frequency representation of the electrogastrogram-application of the exponential-distribution," *IEEE Trans. Biomed. Eng.*, vol. 41, pp. 267–275, Mar. 1994.
[9] Z. Y. Lin and J. D. Chen, "Advances in time-frequency analysis of biomedical signals," *Crit. Rev. Biomed. Eng.*, vol. 24, no. 1, pp. 1–72, 1996.
[10] C. Li, C. Zheng, and C. Tai, "Detection of ECG characteristic points using wavelet transform," *IEEE Trans. Biomed. Eng.*, vol. 42, pp. 21–28, Jan. 1995.
[11] A. Khamene and S. Negahdaripour, "A new method for the extraction of fetal ECG from the composite abdominal signal," *IEEE Trans. Biomed. Eng.*, vol. 47, pp. 507–516, Apr. 2000.
[12] S. K. Setarehdan and J. J. Soraghan, "Automatic cardiac LV boundary detection and tracking using hybrid fuzzy temporal and fuzzy multiscale edge detection," *IEEE Trans. Biomed. Eng.*, vol. 46, pp. 1364–1378, Nov. 1999.
[13] L. M. Bruce and R. R. Adhami, "Classifying mammographic mass shape using the wavelet transform modulus-maxima method," *IEEE Trans. Biomed. Eng.*, vol. 18, pp. 1170–1177, Dec. 1999.
[14] F. H. Y. Chan, B. M. Wu, F. K. lam, P. W. F. Poon, and A. M. S. Poon, "Multiscale characterization of chronobiological signals based on the discrete wavelet transform," *IEEE Trans. Biomed. Eng.*, vol. 47, pp. 88–95, Jan. 2000.
[15] A. Grossmann and J. Morlet, "Decomposition of hardy functions into square integrable wavelets of constant shape," *SIAM J. Math.*, vol. 15, pp. 723–736, 1984.

[16] C. Chui, *An Introduction to Wavelets*. San Diego, CA: Academic., 1992.
[17] S. Mallat and W. L. Hwang, "Singularity detection and processing with wavelets," *IEEE Trans. Inform. Theory*, vol. 38, pp. 617–643, Feb. 1992.
[18] S. Mallat and S. Zhong, "Characterization of signals from multiscale edges," *IEEE Trans. Pattern Anal. Machine Intell.*, vol. 14, pp. 710–732, July 1992.
[19] D. Dubios and H. Prade, *Fuzzy Sets and Systems: Theory and Applications*. New York: Academic and Harcourt Brace Jovanovich, 1980.
[20] D. L. Donoho and I. M. Johnstone, "Adapting to unknown smoothness via wavelet shrinkage," *J. Amer. Stat. Assoc.*, vol. 90, pp. 1200–1224, 1995.
[21] ——, "Ideal spatial adaptation via wavelet shrinkage," *Biometrika*, vol. 81, pp. 425–455, 1994.
[22] M. Knaflitz and R. Merletti, "Suppression of simulation artifacts from myoelectric-evoked potential recordings," *IEEE Trans. Biomed. Eng.*, vol. 35, pp. 758–763, Sept. 1988.

Hualou Liang (SM'00) received the M.Sc. degree in electronic engineering from Dalian University of Technology, Dalian, China, and the Ph.D. degree in physics from the Chinese Academy of Sciences, Beijing, China.

He is an Assistant Professor in University of Texas Health Science Center, Houston, USA. He was Postdoctoral Researcher in Tel-Aviv University, Tel-Aviv, Israel, Max-Planck-Institute for Biological Cybernetics, Tübingen, Germany, and the Center for Complex Systems and Brain Sciences, Florida Atlantic University, Boca Raton. He has written more than 50 papers, conference proceedings, and book chapters. His research experience throughout the years ranges from areas in biomedical signal processing to cognitive and computational neuroscience. He teaches graduate interdisciplinary courses including "Biomedical Signal Processing" and "Computational Biomedicine."

Zhiyue Lin (A'95–SM'97) is currently a Research Scientist in Department of Medicine at University of Kansas Medical Center (KUMC), Kansas City. Prior to working at KUMC, he was a Visiting Scientist at University of Virginia Health Sciences Center, Charlottesville, and was with the Institute of Information Engineering at Dalian University of Technology, Dalian, China, where he has been an Associate Professor since 1990.

He has published over 100 papers and abstracts, eight book chapters, and co-authored one textbook. His research interests include digital signal/image processing and their applications, biomedical signal and information processing, electrophysiology, and functional electrical stimulation.